Int. J. Solids Structures Vol. 29, No. 5, pp. 591–610, 1992
Printed in Great Britain.

0020–7683/92 $5.00 + .00

REFINED BUCKLING AND POSTBUCKLING ANALYSIS OF TWO-DIMENSIONAL DELAMINATIONS—I. ANALYSIS AND VALIDATION†

W.-L. YIN
School of Civil Engineering, Georgia Institute of Technology, Atlanta, GA 30332, U.S.A.

and

K. C. JANE
BMT International, Inc., Columbia, MD 21044, U.S.A.

(*Received* 4 *October* 1990; *in revised form* 16 *June* 1991)

Abstract—An analytical procedure, based on the Rayleigh–Ritz method and von Karman's nonlinear theory of plates, is developed for computing the buckling loads and the postbuckling solutions of laminated anisotropic elliptical plates. Lengthy algebraic equations governing the expansion coefficients of the displacement functions are generated by a symbolic algorithm. Using polynomial displacement expansions of different orders, postbuckling solutions with increasing accuracy are systematically computed for isotropic and laminated elliptical plates. The deflections, the force and moment resultants and the energy release rates associated with the solutions of various orders are compared to assess the trend of convergence. The comparison suggests the lowest order polynomial expansion needed to obtain reasonably accurate results for the force and moment resultants and the energy release rates. Previous Rayleigh-Ritz postbuckling solutions based on lower-order polynomial expansions of the displacements are found to yield results with significant errors.

1. INTRODUCTION

The problems of sublaminate buckling and crack growth in a homogeneous plate or a composite laminate containing an interior delamination have been the subject of extensive analytical and numerical studies in the past decade.‡ For thin strip or elliptical delamination models the bifurcation loads obtained by two- or three-dimensional finite element analysis [see, for example, Shivakumar and Whitcomb (1985) and Yin *et al.* (1986a)] are not appreciably different from the corresponding results of the homogeneous or laminated plate analysis. In the case of strip delamination models, closed-form analytical solutions of the postbuckling deformation may be obtained in the context of the classical laminated plate theory (Chai *et al.*, 1981; Yin *et al.*, 1986b). The energy release rates associated with delamination growth may be evaluated, by using the path-independent J-integral, in terms of the membrane forces and the bending moments in the cracked and intact parts of the laminate at the crack tip (Yin and Wang, 1984). The results also agree well with the energy release rates calculated by finite element analysis and the closure integral method (Yin *et al.*, 1986a). These findings suggest that accurate postbuckling analysis based on a homogeneous or laminated plate theory (preferably with the inclusion of the effect of the thickness–shear deformation) may be used, in place of expensive three-dimensional analysis, to obtain reliable results for the buckling and growth behavior of a delamination with a general shape.

For a two-dimensional thin-film delamination with an arbitrary shape, the local membrane forces and the bending and twisting moments at a point of the delamination front determine the pointwise value of the energy release rate (Bottega, 1983; Storakers and Anderson, 1988). If one assumes a delamination growth criterion depending only on the local energy release rate, without discriminating among its separate components associated

† A preliminary version of this paper was presented in the ASME Winter Annual Meeting, San Francisco, CA, December 1989.

‡ For general reviews of the subject, see the recent articles by Garg (1988) and Storakers (1989). Additional information may be found in Kapania and Raciti (1989), Simitses (1989) and Yin (1989).

with the three fracture modes, then the principal task involved in the analysis of two-dimensional delaminations is that of obtaining accurate bifurcation loads and postbuckling solutions from the von Karman equations. This task is formidable if one wishes to take into account the postbuckling deformations of both the cracked and intact parts of the plate. It is difficult even if one completely ignores the bending deformation and the non-uniformity of the membrane deformation in the base laminate as induced by local buckling of a thin delaminated layer, i.e. if one adopts the "thin-film" approximation for the delaminated layer by imposing the conditions of vanishing deflection and slope along the crack boundary.

The difficulties arise from the geometrical non-linearity and the strong coupling between the in-plane and transverse displacements that are intrinsic to the von Karman equations of plates. Postbuckling solutions which ignore or inadequately account for such effects cannot yield reliable results for the membrane forces, the bending and twisting moments, or the energy release rates. Many existing solution schemes for the bending and buckling of plates use the calculated results of the central deflection as the principal test of accuracy. The criterion is inadequate and misleading because, as shown in this paper, relatively crude postbuckling solutions may yield sufficiently accurate results for the central deflection and, at the same time, very poor results for the membrane forces and the energy release rates.

In their analysis of transversely loaded and postbuckled *rectangular* plates, Chia (1980) and co-workers obtained solutions by the Rayleigh–Ritz method, using beam eigenfunctions to approximate the displacements. As the number of terms in the displacement functions increases, the results for the transverse deflection converge reasonably fast. However, accurate results for the membrane forces and the bending moments are considerably more difficult to obtain. Following Chia's method, Feng (1983) presented a computerized analysis of the postbuckling behavior of laminated anisotropic rectangular plates. His analysis used a much larger set of beam eigenfunctions to represent the displacements of the middle surface. He did not provide information concerning the rate or trend of convergence of the solutions.

In a postbuckling analysis of a simply-supported circular plate under axisymmetric compression, Friedrichs and Stoker (1941, 1942) noticed significant non-uniform membrane deformation in an advanced stage of postbuckling. As the boundary compression increases, the membrane forces in a central portion of the plate eventually become tensile. Bodner (1973) found a similar behavior in the axisymmetric postbuckling of a clamped circular plate. Due to the coupling in the von Karman equations, the non-uniformity of the in-plane deformation has important implications for the bending deformation. This results in large curvature of the deformed middle surface around the boundary of the plate. Although the perturbation method used by these authors is applicable only to within a certain range of the strain load, the general validity of their conclusions beyond this range has been confirmed by an analysis based on direct integration of the von Karman equations (Yin, 1985).

As suggested by Chai and Babcock (1985), the buckling and growth behavior associated with general two-dimensional delaminations may be studied by an analysis of elliptical delaminations. However, the displacement functions used by Chai and Babcock contain an insufficient number of terms to reflect significant non-uniform membrane deformation and the boundary effect. In the present work, power series expansions of the displacements are systematically enlarged to obtain higher order approximate solutions of postbuckled, clamped elliptical plates by means of the Rayleigh–Ritz method. In the special case of axisymmetric postbuckling of circular plates, Rayleigh–Ritz solutions of the various orders are compared with the solutions obtained by direct integration of the von Karman equations (Yin, 1985). The comparison indicates convergence of the Rayleigh–Ritz solutions, and suggests the lowest order approximate solution needed to obtain reasonably accurate results for the membrane forces, the bending moments and the energy release rates. The solutions of the required order are then computed for elliptical delaminations with various aspect ratios. It is found that these postbuckling solutions also show significant boundary effect, although in a manner more complex and fascinating than in the case of axisymmetric postbuckling of circular plates.

A Rayleigh–Ritz procedure involving a relatively large number of coefficients for the non-linear analysis of anisotropic plates requires the use of symbolic algebra. A symbolic computational program is written in the Fortran code to generate the total potential energy function in terms of the geometrical, material and loading parameters, as well as the undetermined expansion coefficients (Jane, 1989). The program also yields the non-linear algebraic equations governing the undetermined coefficients. Solutions of the equations are computed for isotropic circular and elliptical plates (in Part I of this paper) and for cross-ply and angle-ply elliptical laminates (in Part II).

Non-dimensionalization of the postbuckling problem shows that the total potential energy function depends on the geometrical and stiffness parameters through certain specific combinations. Consequently, *all postbuckling solutions of anisotropic elliptical (or rectangular) laminates may be generated from appropriate solutions of anisotropic circular (or square) laminates by rescaling variables*. This important conclusion, shown in Section 2.3 of the present paper, allows a significant saving of computational effort in a parametric study of the postbuckling behavior of various types of elliptical laminates.

2. RAYLEIGH–RITZ SOLUTIONS

We consider an elliptical delamination with semi-axial lengths a and b along the X- and Y-coordinate axes, respectively. Let the base plate be subjected to uniform in-plane normal and shearing strains E_{XX}, E_{YY} and E_{XY}. If the strains are predominantly compressive and if they are sufficiently large, then the elliptical delaminated layer buckles and becomes completely or partially detached from the base plate. We assume that the thickness of the delaminated layer, h, is small compared to the thickness of the base plate, so that, within the base plate, the bending deformation and the non-uniformity of the in-plane deformation caused by the buckling of the delaminated layer are both negligibly small. Then the delaminated layer is subjected to displacement boundary conditions along the entire elliptical boundary. The total potential energy of the layer is identical to its total strain energy.

2.1. *The total potential energy*

In the buckled states, the membrane strains and the curvatures of the middle surface of the delaminated layer may be approximated by

$$\varepsilon_1 = \frac{\partial U}{\partial X} + \frac{1}{2}\left(\frac{\partial W}{\partial X}\right)^2, \quad \varepsilon_2 = \frac{\partial V}{\partial Y} + \frac{1}{2}\left(\frac{\partial W}{\partial Y}\right)^2, \quad \varepsilon_6 = \frac{\partial U}{\partial Y} + \frac{\partial V}{\partial X} + \frac{\partial W}{\partial X}\frac{\partial W}{\partial Y}$$

$$\kappa_1 = \frac{\partial^2 W}{\partial X^2}, \quad \kappa_2 = \frac{\partial^2 W}{\partial Y^2}, \quad \kappa_6 = 2\frac{\partial^2 W}{\partial X \partial Y} \tag{1}$$

where U and V are the in-plane displacements on the middle surface and where W is the transverse deflection. The force and moment resultants of the delaminated layer are related to the strains and the curvatures according to the equation

$$\begin{Bmatrix} N_1 \\ N_2 \\ N_6 \\ M_1 \\ M_2 \\ M_6 \end{Bmatrix} = \begin{bmatrix} A_{11} & A_{12} & A_{16} & B_{11} & B_{12} & B_{16} \\ A_{12} & A_{22} & A_{26} & B_{12} & B_{22} & B_{26} \\ A_{16} & A_{26} & A_{66} & B_{16} & B_{26} & B_{66} \\ B_{11} & B_{12} & B_{16} & D_{11} & D_{12} & D_{16} \\ B_{12} & B_{22} & B_{26} & D_{12} & D_{22} & D_{26} \\ B_{16} & B_{26} & B_{66} & D_{16} & D_{26} & D_{66} \end{bmatrix} \begin{Bmatrix} \varepsilon_1 \\ \varepsilon_2 \\ \varepsilon_6 \\ \kappa_1 \\ \kappa_2 \\ \kappa_6 \end{Bmatrix}.$$

The stiffness coefficients in the last equation are those defined in the classical laminated plate theory. If we abbreviate the preceding equation in the form

$$N_i = A_{ij}\varepsilon_j + B_{ij}\kappa_j, \quad M_i = B_{ij}\varepsilon_j + D_{ij}\kappa_j \tag{2}$$

then the total potential energy of the delaminated layer may be expressed as

$$\Pi = \frac{1}{2}\int\int \sum_i (N_i\varepsilon_i + M_i\kappa_i)\, \mathrm{d}X\, \mathrm{d}Y \tag{3}$$

where the integration is carried over the region of the plate and the index i is summed over 1, 2 and 6.

2.2. *Non-dimensionalization and polynomial approximation*

We introduce the following non-dimensional variables and constants:

$$\begin{gathered} x \equiv X/a, \quad u \equiv Ua/h^2, \quad w \equiv W/h, \\ y \equiv Y/b, \quad v \equiv Vb/h^2, \quad \lambda \equiv a/b, \end{gathered} \qquad \bar{\Pi} \equiv \frac{2(a/h)^4}{A_{11}ab}\Pi$$

$$\varepsilon_{xx} \equiv (a/h)^2 E_{XX}, \quad \varepsilon_{xy} \equiv (ab/h^2)E_{XY}, \quad \varepsilon_{yy} = (b/h)^2 E_{YY}$$

$$\bar{\varepsilon}_1 = (a/h)^2\varepsilon_1, \quad \bar{\varepsilon}_2 = (b/h)^2\varepsilon_2, \quad \bar{\varepsilon}_6 = (ab/h^2)\varepsilon_6$$

$$\bar{\kappa}_1 = (a^2/h)\kappa_1, \quad \bar{\kappa}_2 = (b^2/h)\kappa_2, \quad \bar{\kappa}_6 = (ab/h)\kappa_6. \tag{4}$$

Let the displacement functions be approximated by the polynomial expansions

$$\begin{aligned} U &= axE_{XX} + byE_{XY} + (1-x^2-y^2)P(x,y)h^2/a \\ V &= axE_{XY} + byE_{YY} + (1-x^2-y^2)Q(x,y)h^2/b \\ W &= h(1-x^2-y^2)^2 R(x,y) \end{aligned}$$

where P, Q and R are polynomial functions of the normalized coordinate variables. All boundary conditions along $(X/a)^2 + (Y/b)^2 = 1$ are satisfied by these displacement functions. Now the non-dimensional displacement components u, v and w have the following expressions:

$$\begin{aligned} u &= x\varepsilon_{xx} + y\varepsilon_{xy} + Z_0 P(x,y) \\ v &= x\varepsilon_{xy} + y\varepsilon_{yy} + Z_0 Q(x,y) \\ w &= Z_0^2 R(x,y), \end{aligned} \tag{5}$$

where

$$Z_0 \equiv 1 - x^2 - y^2.$$

From eqn (1) we obtain the following expressions for the normalized membrane strain components and the normalized curvatures

$$\begin{aligned} \bar{\varepsilon}_1 &= \varepsilon_{xx} + (Z_0 P)_{,x} + (1/2)[(Z_0^2 R)_{,x}]^2 \\ \bar{\varepsilon}_2 &= \varepsilon_{yy} + (Z_0 Q)_{,y} + (1/2)[(Z_0^2 R)_{,y}]^2 \\ \bar{\varepsilon}_6 &= 2\varepsilon_{xy} + (Z_0 P)_{,y} + (Z_0 Q)_{,x} + (Z_0^2 R)_{,x}(Z_0^2 R)_{,y} \\ \bar{\kappa}_1 &= (Z_0^2 R)_{,xx}, \quad \bar{\kappa}_2 = (Z_0^2 R)_{,yy}, \quad \bar{\kappa}_6 = 2(Z_0^2 R)_{,xy}. \end{aligned}$$

The polynomials P, Q and R are defined by their respective sets of coefficients $\{a_i\}$, $\{b_i\}$ and $\{c_i\}$. The number of coefficients in each set depends on the degree of the polynomial. We define twenty-one functions L_{ij}, M_{ij} and N_{ij} ($i, j = 1, 2, 6$; L_{ij} and N_{ij} are symmetric

with respect to the indices while M_{ij} is not) by the following integrals over the unit disk $x^2+y^2 \leqslant 1$:

$$L_{ij} = \iint \bar{\varepsilon}_i \bar{\varepsilon}_j \, dx \, dy, \quad M_{ij} = \iint \bar{\varepsilon}_i \bar{\kappa}_j \, dx \, dy, \quad N_{ij} = \iint \bar{\kappa}_i \bar{\kappa}_j \, dx \, dy. \tag{6}$$

It is clear that L_{ij}, M_{ij} and N_{ij} depend only on the normalized strain loads ε_{xx}, ε_{yy}, ε_{xy} and the coefficients $\{a_i\}$, $\{b_i\}$ and $\{c_i\}$ of the polynomials P, Q and R. Thus, once the forms of the polynomials P, Q and R are selected, all the integrals L_{ij}, M_{ij} and N_{ij} can be evaluated and expressed *explicitly* in terms of the normalized strain loads in the base plate and the coefficients of the polynomials. These explicit expressions are *independent* of the geometrical and material parameters (a, b, h, A_{ij}, B_{ij}, D_{ij}) of the anisotropic elliptical plate. They depend only on the approximation scheme used in the analysis.

Equation (3) now yields the following expression for the non-dimensional potential energy:

$$\bar{\Pi} = \frac{(a/h)^4}{A_{11}} \sum_i \sum_j \delta_i \delta_j [A_{ij} L_{ij} + (2/h) B_{ij} M_{ij} + (1/h^2) D_{ij} N_{ij}] \tag{7}$$

where i and j are again summed over 1, 2 and 6 and

$$\delta_1 = (h/a)^2, \quad \delta_2 = (h/b)^2, \quad \delta_6 = h^2/ab.$$

Once an approximating scheme involving a set of undetermined coefficients a_i, b_i and c_i is adopted and the integrals L_{ij}, M_{ij} and N_{ij} are explicitly obtained, the total potential energy for any particular geometrical and material configuration of the elliptical laminate can be obtained straightforwardly. This yields an expression for the normalized potential energy:

$$\bar{\Pi} = \bar{\Pi}(a_i, b_i, c_i, \varepsilon_{xx}, \varepsilon_{yy}, \varepsilon_{xy}; \lambda, A_{ij}/A_{11}, B_{ij}/hA_{11}, D_{ij}/h^2 A_{11}). \tag{8}$$

It is clear that the major task involved in the explicit determination of the last expression is that of evaluating the integrals of eqn (6). Each integral is a sum of integrals of the following form:

$$I(m,n,k) = \int_{-1}^{1} \int_{-(1-y^2)^{1/2}}^{(1-y^2)^{1/2}} x^m y^n (1-x^2-y^2)^k \, dx \, dy$$

$$= \int_0^1 (1-r^2)^k r^{m+n+1} \, dr \int_0^{2\pi} \cos^m \theta \sin^n \theta \, d\theta.$$

One has $I(m, n, k) = 0$ if m and n are not both even. Otherwise,

$$I(m,n,k) = 2\pi \cdot \frac{1 \cdot 3 \cdot 5 \cdots (m-1) \cdot 1 \cdot 3 \cdot 5 \cdots (n-1)}{2 \cdot 4 \cdot 6 \cdots (m+n)} \cdot \sum_{p=0}^{k} \frac{(-1)^p k!}{(2+2p+m+n) p! (k-p)!}.$$

Depending on the number of coefficients involved in the polynomials P, Q and R, the final approximate expression for the potential energy may contain hundreds or even thousands of terms. The intermediate steps leading to the final expression may involve hundreds of thousands of integrals. A special purpose symbolic algorithm was developed in the Fortran code to generate the potential energy function and the algebraic equations governing the undetermined coefficients (Jane, 1989). Cyber 205 supercomputer at the University of Georgia was used to implement the symbolic algorithm and to solve the resulting system of non-linear algebraic equations. This system consists of the following equations

$$\frac{\partial \bar{\Pi}}{\partial a_i} = 0, \quad \frac{\partial \bar{\Pi}}{\partial b_i} = 0, \quad \frac{\partial \bar{\Pi}}{\partial c_i} = 0. \tag{9}$$

Furthermore, the strains in the base plate corresponding to the states of bifurcation (from membrane states to buckled states) may be calculated from the following characteristic equation

$$\begin{vmatrix} \frac{\partial^2 \bar{\Pi}}{\partial a_i \partial a_j} & \frac{\partial^2 \bar{\Pi}}{\partial a_i \partial b_j} & \frac{\partial^2 \bar{\Pi}}{\partial a_i \partial c_j} \\ \frac{\partial^2 \bar{\Pi}}{\partial b_i \partial a_j} & \frac{\partial^2 \bar{\Pi}}{\partial b_i \partial b_j} & \frac{\partial^2 \bar{\Pi}}{\partial b_i \partial c_j} \\ \frac{\partial^2 \bar{\Pi}}{\partial c_i \partial a_j} & \frac{\partial^2 \bar{\Pi}}{\partial c_i \partial b_j} & \frac{\partial^2 \bar{\Pi}}{\partial c_i \partial c_j} \end{vmatrix}_{(a_i = b_i = c_i = 0)} = 0. \tag{10}$$

Equation (9) will be solved for the coefficients $\{a_i\}$, $\{b_i\}$ and $\{c_i\}$ by using the Newton–Raphson iteration scheme. In order to have suitable initial estimates of the coefficients, it is imperative to start from a bifurcation point (corresponding to a set of coefficients satisfying eqn (10)) in the load space, and to obtain successive postbuckling solutions along a load path by imposing small load increments. The coordinates of the load space are the imposed in-plane normal and shearing strains in the base plate. Since eqn (9) consists of algebraic equations which depend linearly on the coefficients $\{a_i\}$ and $\{b_i\}$, the emphasis in each iteration step is to obtain the proper increment of $\{c_i\}$. The new iterated values of $\{a_i\}$ and $\{b_i\}$ may be obtained easily by solving a subsystem of linear equations using the current estimates of $\{c_i\}$.

2.3. *Generating all postbuckling solutions of elliptical laminates from appropriate solutions of circular laminates by rescaling*

The structure of the expression for the total potential energy, eqn (7), implies the following important conclusion: all postbuckling solutions of elliptical laminates (according to the von Karman theory) may be obtained from the postbuckling solutions of circular laminates by rescaling the coordinate variables, the thickness, the stiffness parameters and the membrane strain loads. Indeed, if one wants to obtain the postbuckling solution U, V, W of an elliptical laminate with the thickness h, semi-axial lengths a and b, stiffness matrices $[A_{ij}]$, $[B_{ij}]$ and $[D_{ij}]$, under the strain loads E_{XX}, E_{YY} and E_{XY} in the base plate, one only has to obtain the solution U_0, V_0, W_0 of a circular laminate with the thickness h_0, radius r_0 and stiffness coefficients

$$\begin{aligned} S^0_{11} &= (r_0/h_0)^4(h/a)^4 S_{11}, & S^0_{12} &= (r_0/h_0)^4(h^2/ab)^2 S_{12} \\ S^0_{22} &= (r_0/h_0)^4(h/b)^4 S_{22}, & S^0_{16} &= (r_0/h_0)^4(h^4/a^3 b) S_{16} \\ S^0_{66} &= (r_0/h_0)^4(h^2/ab)^2 S_{66}, & S^0_{26} &= (r_0/h_0)^4(h^4/ab^3) S_{26} \end{aligned}$$

(where S_{ij} stands for A_{ij}, B_{ij} and D_{ij} in succession) under the strain loads

$$E^0_{XX} = (h_0/r_0)^2(a/h)^2 E_{XX}, \quad E^0_{YY} = (h_0/r_0)^2(b/h)^2 E_{YY}, \quad E^0_{XY} = (h_0/r_0)^2(ab/h^2) E_{XY}.$$

The solution for the elliptical laminate is related to the solution of the circular laminate by

$$U = (h/h_0)^2(r_0/a)U_0, \quad V = (h/h_0)^2(r_0/b)V_0, \quad W = (h/h_0)W_0.$$

The validity of this statement follows from the fact that the two laminates have the same $\delta_i\delta_j A_{ij}$, $\delta_i\delta_j B_{ij}$ and $\delta_i\delta_j D_{ij}$, the strain loads on the respective laminates have the same normalized values ε_{xx}, ε_{yy} and ε_{xy}, and the respective solutions have the same normalized displacements u, v and w. From eqn (7) one finds that the potential energy functions of the

two laminates are identical except for a multiplicative factor. Hence the stationary condition for the respective potential energies are realized by the same normalized displacement solution u, v and w.

Since one has the freedom to choose the radius r_0 and the thickness h_0 of the circular laminate arbitrarily, there are infinitely many postbuckling solutions of circular laminates which correspond, according to the preceding relations, to the same postbuckling solution of a given elliptical laminate. Furthermore, one may introduce new rectangular coordinate axes in such a way that, for the circular laminate, these axes coincide with the principal directions of the imposed strain tensor in the base plate (whose components in the original coordinates are E^0_{XX}, E^0_{YY} and E^0_{XY}). Referred to the new coordinate system the strain load in the base plate of the circular laminate has no shearing component. Consequently, in a parametric study of the postbuckling behavior of elliptical delaminations of various geometrical and material configurations under general membrane strain loads in the base plate, it is sufficient to deal only with *circular* anisotropic delaminations under biaxial strain loads. All solutions of the elliptical delaminations may be generated from appropriate solutions of circular delaminations according to the preceding rescaling rules.

It is clear that a similar procedure may be used to generate all postbuckling solutions of rectangular anisotropic laminates from appropriate solutions of square laminates subjected to general in-plane loads.

2.4. *Symmetry conditions on the displacement functions*

For a general anisotropic elliptical delamination in a base plate under the in-plane strain loads E_{XX}, E_{YY} and E_{XY}, the postbuckling displacement functions in the delaminated sublaminate satisfy the conditions of central symmetry:

$$u(-x,-y) = -u(x,y), \quad v(-x,-y) = -v(x,y), \quad w(-x,-y) = w(x,y). \tag{11}$$

These symmetry conditions imply that the polynomials P and Q in eqn (5) contain only terms of odd degrees while the polynomial R contains only terms of even degrees. In the cases of isotropic, specially orthotropic, or cross-ply sublaminates with aligned loading and symmetry axes, additional symmetry conditions with respect to the coordinate axes apply:

$$\begin{aligned} u(x,y) &= -u(-x,y) = u(x,-y), \\ v(x,y) &= v(-x,y) = -v(x,-y), \\ w(x,y) &= w(-x,y) = w(x,-y). \end{aligned} \tag{12}$$

Equations (11) and (12) taken together imply that P, Q and R have the forms

$$P(x,y) = xP_1(x^2,y^2), \quad Q(x,y) = yQ_1(x^2,y^2), \quad R(x,y) = R_1(x^2,y^2). \tag{13}$$

If P_1 and Q_1 include only constant terms and R_1 includes, in addition, linear terms in x_2 and y_2, then the displacement functions reduce to those used by Chai and Babcock (1985) in their five-term Rayleigh–Ritz solutions. Rayleigh–Ritz solutions of higher orders $\{p, r\}$ may be considered where p and r refer, respectively, to the degrees of the polynomials P (same as that of Q) and R of eqn (5). For example, for the solution of the order $\{5, 4\}$ satisfying the full symmetry conditions of eqns (11) and (12), the polynomials P, Q and R of eqn (5) have the following forms:

$$\begin{aligned} P(x,y) &= x(a_1 + a_2x^2 + a_3y^2 + a_4x^4 + a_5x^2y^2 + a_6y^4) \\ Q(x,y) &= y(b_1 + b_2x^2 + b_3y^2 + b_4x^4 + b_5x^2y^2 + b_6y^4) \\ R(x,y) &= c_1 + c_2x^2 + c_3y^2 + c_4x^4 + c_5x^2y^2 + c_6y^4. \end{aligned} \tag{14}$$

The Rayleigh–Ritz solutions examined in the present work are of the orders $\{1, 2\}$,

{3, 4}, {5, 4}, {5, 6} and {7, 6}. The highest degree of the polynomial and the total number of undetermined coefficients for each order of solutions are shown in Table 1.

In the remaining sections of this paper (Part I), we obtain and examine postbuckling solutions of homogeneous isotropic circular and elliptical plates. These solutions possess the full symmetry properties of eqns (11) and (12). Postbuckling solutions of anisotropic elliptical sublaminates generally satisfy eqn (11) only and their displacement expansions include a considerably larger number of terms, as indicated in Table 1. Such solutions are presented in Part II.

3. CLAMPED ISOTROPIC CIRCULAR PLATES UNDER AXISYMMETRIC COMPRESSION

In a previous work (Yin, 1985), axisymmetric postbuckling solutions of a clamped isotropic circular plate have been obtained by numerical integration of the governing differential equations. These solutions may be used as the standard of comparison for the Rayleigh–Ritz solutions of various orders. The comparison was made over a range of the strain load from the bifurcation strain to about ten times the bifurcation strain. This wide range of the strain load far exceeds the usual range considered in existing postbuckling analyses or appropriate to most practical applications. The intention is to set an extremely severe test of the validity of the lower order approximate solutions by comparing the results with the higher order solutions, and with the solutions obtained by direct integration (Yin, 1985; hereafter called the "reference solutions"), at widely different levels of the strain load. This accounts for the very significant discrepancies in the results shown in the following figures of this paper.

3.1. *Central deflection, membrane force and bending moment*

Consider a circular sublaminate of radius a and thickness h, made of a homogeneous, isotropic elastic material with Young's modulus E and Poisson's ratio ν. The sublaminate has the bending rigidity $D = Eh^3/12(1-\nu^2)$. In an axisymmetric deformation, the radial membrane force and the radial bending moment are related to the radial and transverse displacements, U_r and W, according to the formulae

$$N_r = \frac{Eh}{(1-\nu^2)}\left(\frac{\mathrm{d}U_r}{\mathrm{d}r} + \nu\frac{U_r}{r}\right), \quad M_r = D\left(\frac{\mathrm{d}^2W}{\mathrm{d}r^2} + \frac{\nu}{r}\frac{\mathrm{d}W}{\mathrm{d}r}\right).$$

The strain load in the base plate is given by

$$E_{XX} = E_{YY} = -\varepsilon_0, \quad E_{XY} = 0.$$

We define the non-dimensional compressive radial force and the non-dimensional bending moment as follows:

$$P(\xi) = -\frac{N_r a^2}{D} = 12\left(\frac{\mathrm{d}u}{\mathrm{d}\xi} + \frac{u}{\xi}\right), \quad M(\xi) = \frac{a^2}{hD}M_r = \frac{\mathrm{d}^2w}{\mathrm{d}\xi^2} + \frac{1}{\xi}\frac{\mathrm{d}w}{\mathrm{d}\xi}$$

where a is the radius of the circular plate, w is as defined in eqn (4), and

Table 1. Rayleigh–Ritz solutions of various orders

Solution label	{1, 2}	{3, 4}	{5, 4}	{5, 6}	{7, 6}
Max. degree of P & Q	1	3	5	5	7
Max. degree of R	2	4	4	6	6
Number of coefficients, when eqn (12) does not apply	8	21	33	40	56
Number of coefficients, when eqn (12) applies	5	12	18	22	30

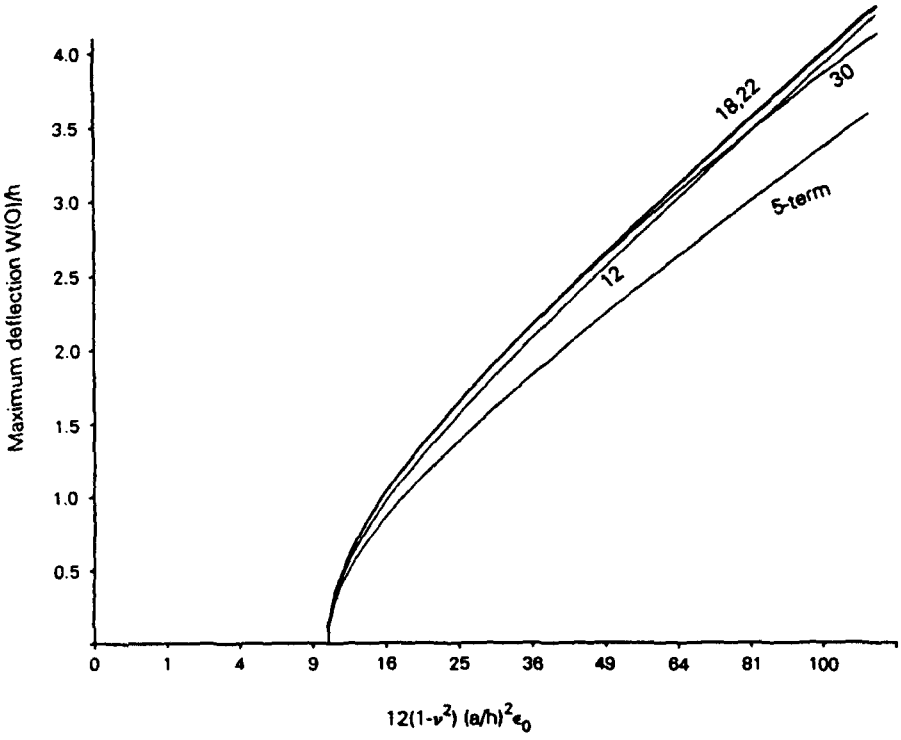

Fig. 1. Circular delamination—deflection at the center.

$$\xi = r/a, \quad u(\xi) = aU_r/h^2, \quad u(1) = -(a/h)^2\varepsilon_0.$$

It is found that, with regard to the central deflection and the radial bending moment at the boundary, Rayleigh-Ritz solutions of the order $\{5, 4\}$ or higher are in excellent agreement with the reference solutions (see Figs 1 and 2, where the solutions of the various

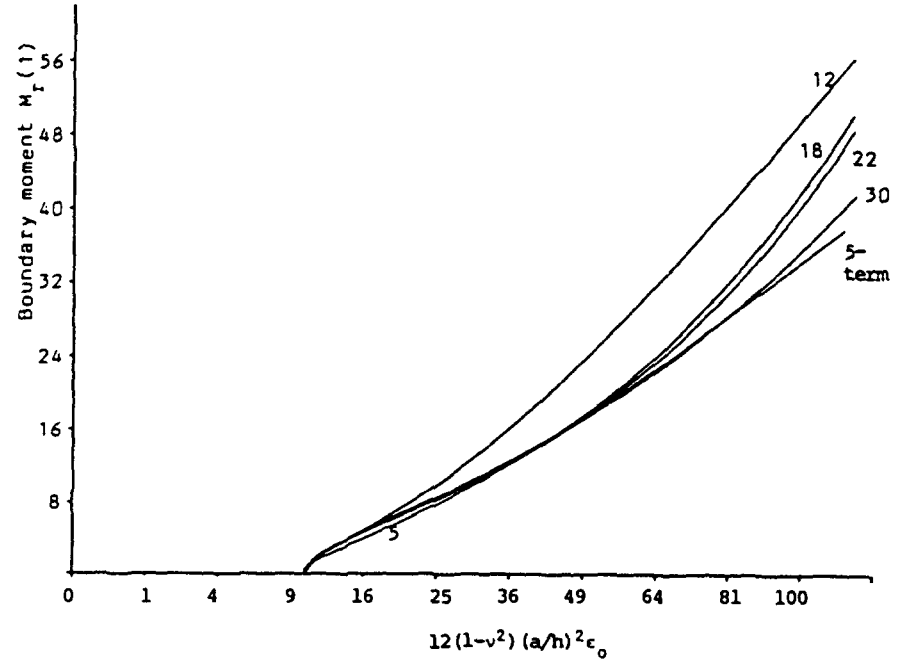

Fig. 2. Circular delamination—boundary radial moment.

orders are identified by the number of coefficients given in the last row of Table 1). The curves associated with the solution of the order $\{7, 6\}$, i.e. the 30-term solution, are nearly indistinguishable from those of the reference solutions. Only the solution of the order $\{7, 6\}$ includes polynomial terms of sufficiently high degree to yield very close results for the boundary radial force, and this is true only in a range of the strain load up to about two to three times the bifurcation strain (Fig. 3). The solutions of the lowest orders, $\{1, 3\}$ and $\{3, 4\}$, generally show very significant errors in the membrane forces.

Strong non-uniformity of the membrane force is indicated by the difference between the radial forces at the boundary (Fig. 3) and at the center (Fig. 4). Under large postbuckling loads, all solutions except the lowest order, $\{1, 3\}$, show tensile radial force at the center. Generally speaking, the solutions of the orders $\{5, 4\}$, $\{5, 6\}$ and $\{7, 6\}$ yield acceptable results (i.e. with about 5% or smaller errors) for the deflections, membrane forces and boundary bending moments over a range of the radial strain load up to about three times the bifurcation strain. When the strain load exceeds this range, the deflection at the center is more than 1.5 times the thickness of the sublaminate (see Fig. 1). Compared with the solutions of the order $\{7, 6\}$, those of the orders $\{5, 4\}$ and $\{5, 6\}$ show significantly larger deviations from the reference solutions.

A comparison of the solutions of the orders $\{5, 4\}$ and $\{5, 6\}$ indicates that, by raising the degree r of the even polynomial R without at the same time also raising the degree p of the odd polynomials P and Q, one increases the number of expansion coefficients in the solution but obtains slight change or improvement in the accuracy of approximation. This is because a satisfactory representation of the non-uniformity of the membrane deformation requires polynomial functions P and Q of sufficiently high degree, and such non-uniformity significantly affects the transverse deflection through the coupling in the von Karman equations.

3.2. *Energy release rates in delamination growth*

For the particular problem at hand, let the total potential energy of the isotropic circular sublaminate be non-dimensionalized in the following manner

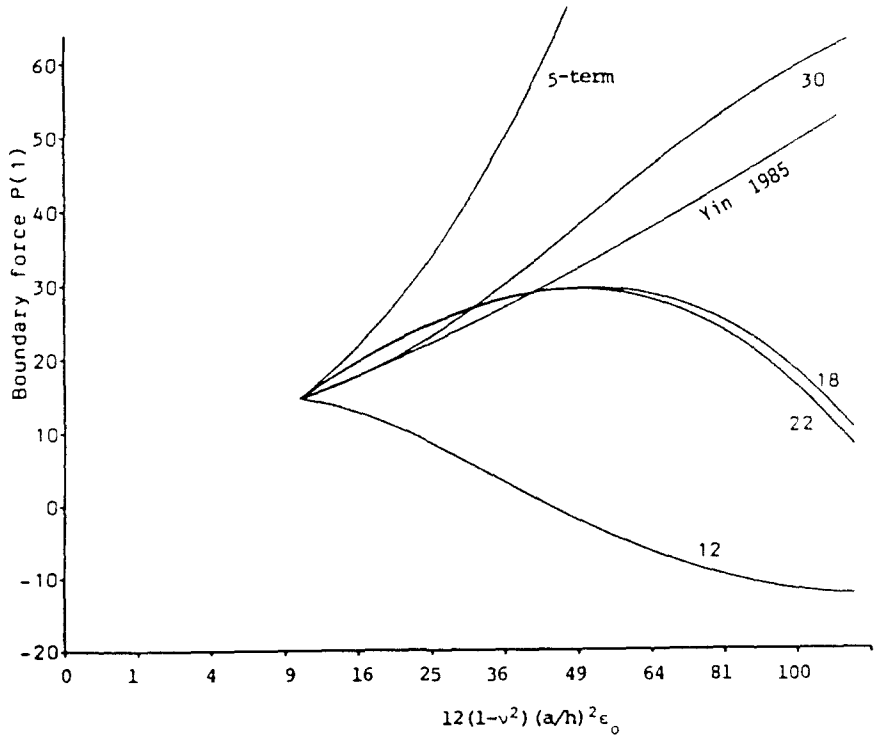

Fig. 3. Circular delamination—radial force at boundary.

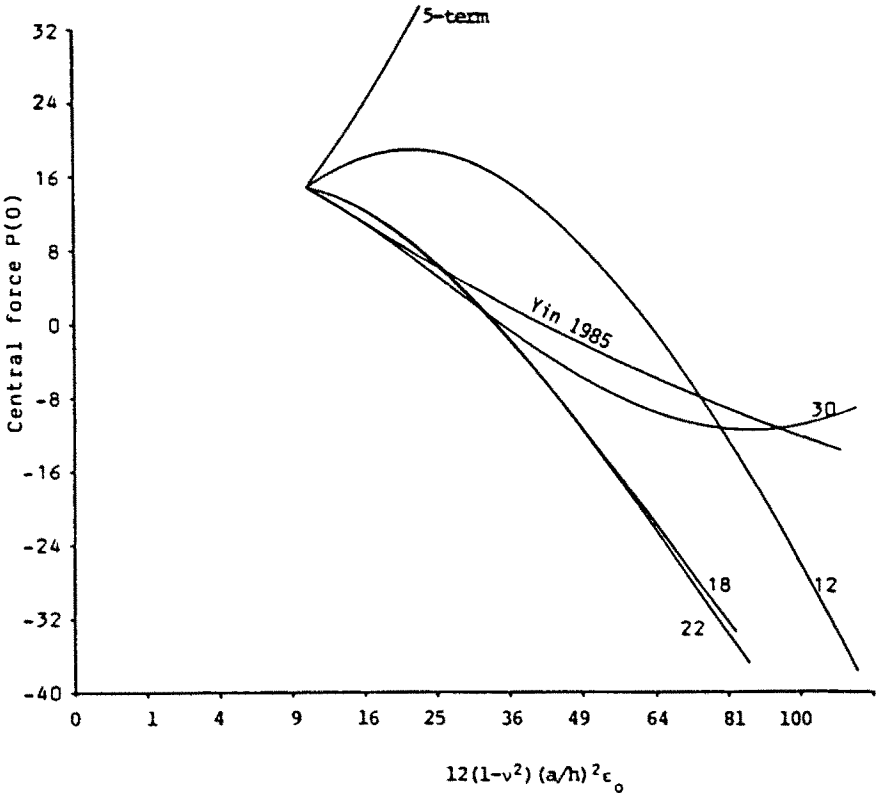

Fig. 4. Circular delamination—membrane force at the center.

$$\bar{\Pi} = (2a^2/\pi Eh^5)\Pi.$$

For the various postbuckling solutions of the sublaminate, the normalized potential energies are plotted in Fig. 5. In this and the two subsequent figures, the horizontal coordinate

$$\sqrt{12(1-\nu^2)}\varepsilon_0(a/h)$$

is interpreted as a normalized delamination radius (under a fixed radial strain load ε_0 in the base plate), rather than as a non-dimensionalized strain load (for a fixed delamination radius a). Under a fixed strain load, the potential energy for an approximate solution may be differentiated with respect to the delamination radius. The result is related to the energy release rate in axisymmetric growth of the delamination according to the following formula

$$\mathcal{G} = \frac{Eh\varepsilon_0^2}{1-\nu} - \frac{1}{2\pi a}\frac{d\Pi}{da}. \tag{15}$$

Comparison of the curves in Figs 5 and 6 indicate that all solutions except the lowest-order yield close results for the potential energies and the energy release rates, while the lowest order solution underestimates the energy release rate by as much as 35%.

The energy release rate may also be evaluated by means of the path-independent M-integral in terms of the boundary radial force and the boundary bending moment of the postbuckling solution (Yin, 1985). This yields the formula

$$G = \frac{1-\nu^2}{2Eh}\left\{\left(\frac{Eh\varepsilon_0}{1-\nu}+N_r(a)\right)^2+12\left(\frac{M_r(a)}{h}\right)^2\right\}. \tag{16}$$

For an exact postbuckling solution the result should agree with the previous result obtained by differentiation of the total potential energy. However, for an approximate postbuckling

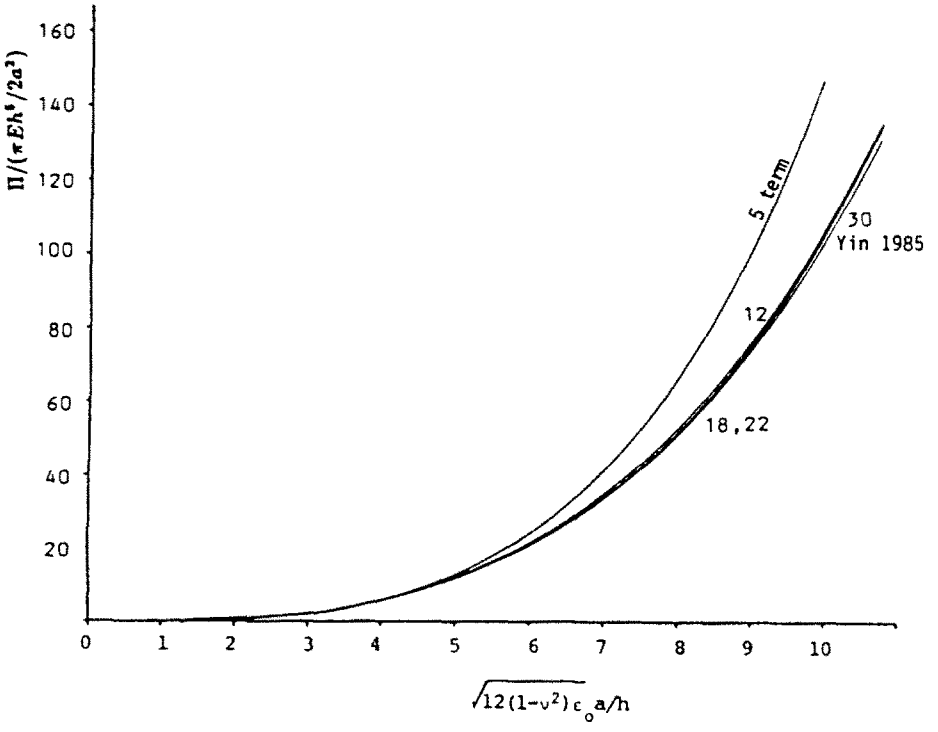

Fig. 5. Circular delamination—potential energy versus the radius.

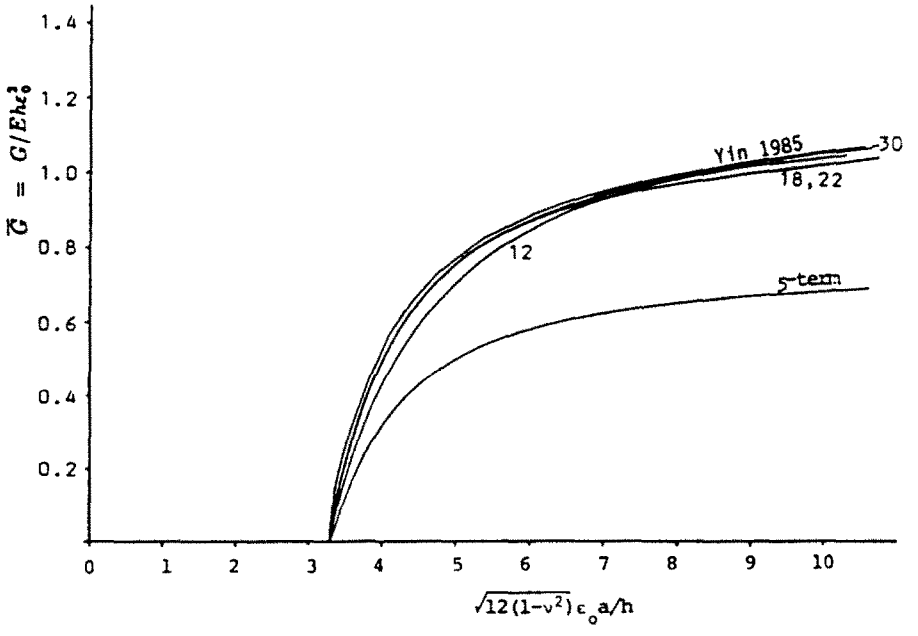

Fig. 6. Energy release rate calculated by differentiating the potential energy with respect to the radius.

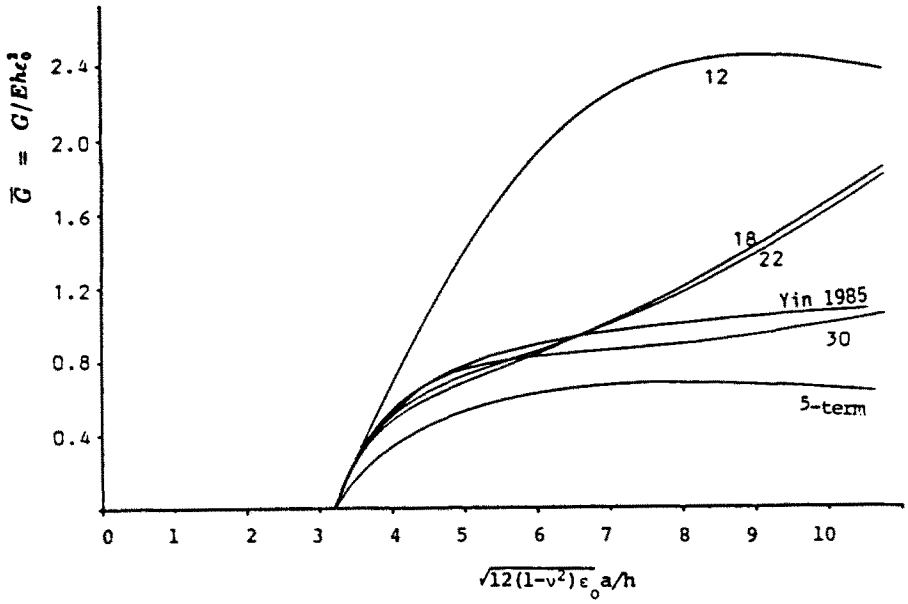

Fig. 7. Energy release rate by the J-integral method.

solution the two results may differ. For the Rayleigh–Ritz solutions of the various orders, the results from eqn (16) are normalized with respect to $Eh\varepsilon_0^2$ and shown in Fig. 7. It is seen that the solutions of the order $\{5, 4\}$ or higher yield close results over a range of strain loads up to about three times the bifurcation strain.

4. ELLIPTICAL DELAMINATIONS

We next obtain the bifurcation loads and the postbuckling solutions of homogeneous isotropic elliptical plates with various aspect ratios by the Rayleigh–Ritz method.

4.1. *Bifurcation loads under equal biaxial compression*

Under equal biaxial loading along the principal axes of the ellipse (i.e. $E_{xx} = E_{yy} = -\varepsilon_0$), the normalized bifurcation loads have been calculated by Woinowsky-Krieger (1937) using elliptical coordinates. His results are shown in Table 2, along with two sets of Rayleigh–Ritz solutions obtained in the present analysis. One set of Rayleigh–Ritz solutions uses a polynomial $R(x, y)$ for $w(x, y)$ containing quadratic and constant terms only. In the second set of solutions, $R(x, y)$ contains quartic and lower-order terms. Since the solutions in a displacement formulation yield upper bounds of the buckling load, the present results, being smaller in value, are better estimates. Furthermore, in the case of a circular delamination ($a/b = 1$), the normalized buckling load predicted by the second set of Rayleigh–Ritz solutions is almost indistinguishable from the exact result, namely, 14.683. As the aspect ratio a/b becomes large, the present upper-bound estimates approach the limiting value $\pi^2 = 9.870$ much faster than the results of Woinowsky-Krieger (1937). Hence the bifurcation loads of elliptical plates under equal biaxial compression are accurately predicted by the Rayleigh–Ritz method involving a small number of expansion coefficients.

Table 2. Normalized buckling loads $P(b^2/D)$ for elliptical delaminations: Comparison of the results of Woinowsky-Krieger (1937) with Rayleigh–Ritz solutions

a/b	1.0	1.4	2.0	3.0	4.0	5.0
Woinowsky-Krieger (1937)	14.79	11.81	11.02	11.01	11.15	11.30
Quadratic R	14.702	11.589	10.517	10.239	10.265	10.32
Quartic R	14.683	11.562	10.436	10.002	9.929	9.955

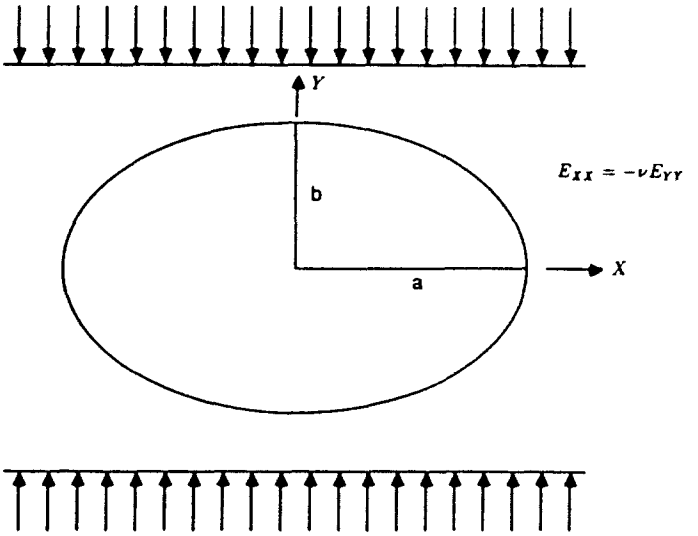

Fig. 8. Elliptical delamination—base plate under uniaxial load.

4.2. *Postbuckling solution under uniaxial compression*

For the postbuckling analyses we consider elliptical delaminations of aspect ratios $a/b = 1$, 2 and 4 in a base plate under membrane strain loads

$$E_{YY} = -\varepsilon_0, \quad E_{XX} = \nu\varepsilon_0, \quad E_{XY} = 0.$$

Such strain loads correspond to *uniaxial* compressive forces applied to the base plate along the Y-direction (Fig. 8). Under a normalized strain load $E_{YY}(b/h)^2 = 4$, and with the assumption $\nu = 0.3$, the in-plane and transverse displacements along the principal axes of the sublaminate are shown in Figs 9–12 for an elliptical sublaminate with $a/b = 2$. Additional figures for the cases $a/b = 1$ and 4 may be found in Jane (1989). Figures 9 and 10 show the deviations of the in-plane displacements in the delaminated layer from the

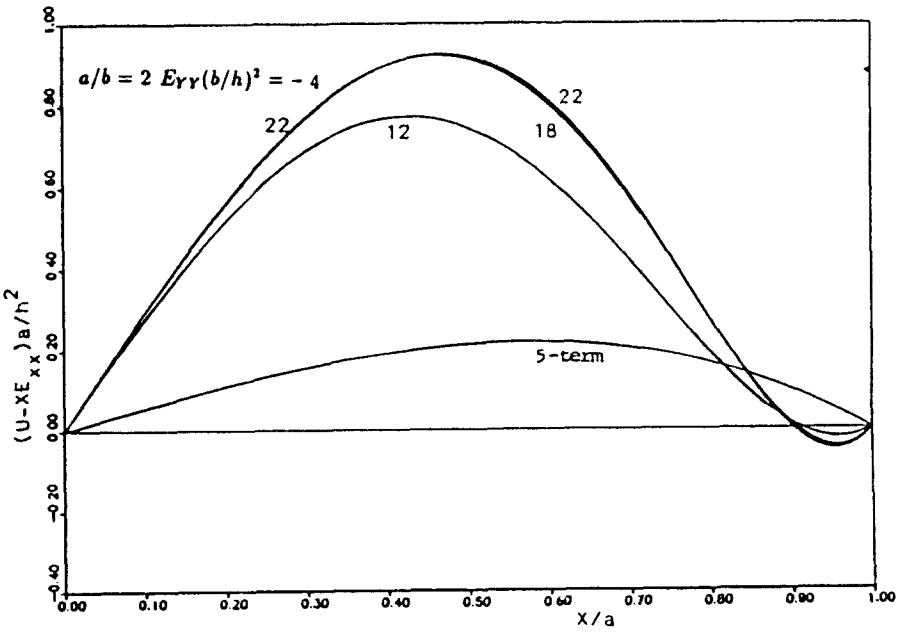

Fig. 9. Displacement U along the X-axis ($a/b = 2$).

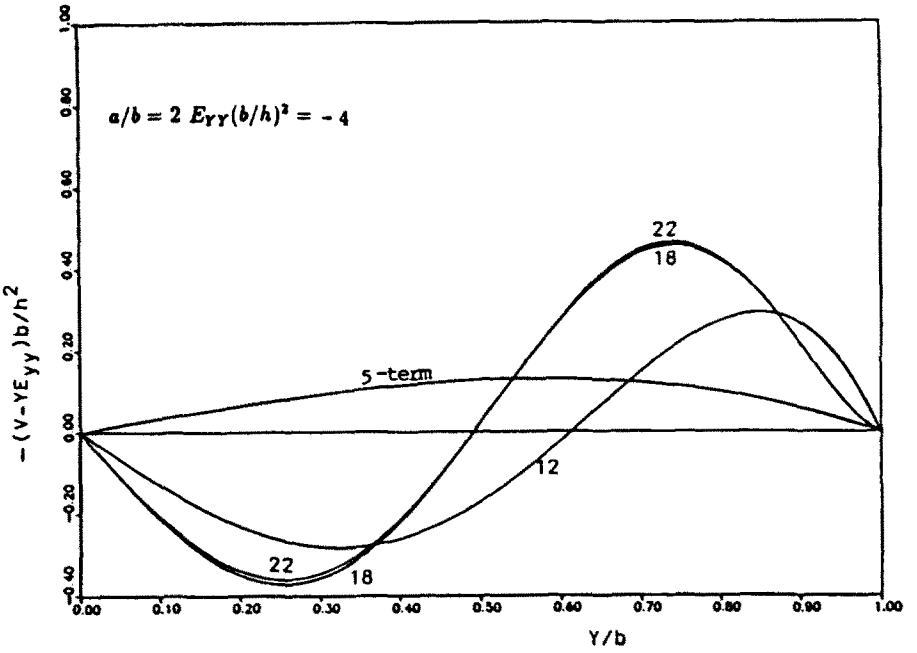

Fig. 10. Displacement V along the Y-axis ($a/b = 2$).

corresponding displacements in the base plate (where, according to the thin-film assumption, the membrane strains are uniform). The slopes of the curves in these figures indicate the deviations of the displacement gradients from the average membrane strains. The results for the solutions of orders $\{5, 4\}$ and $\{5, 6\}$, based on the same polynomial expansions for the in-plane displacements but different expansions for the deflection, are indistinguishable. The significant non-uniformity in the membrane strains shown by these higher-order Rayleigh–Ritz solutions is grossly underestimated by the lowest-order solution. Near the boundary point $(X, Y) = (a, 0)$ the results of the latter are not even qualitatively correct. The non-uniformity in the membrane strains increases with the imposed strain load and with the aspect ratio of the ellipse.

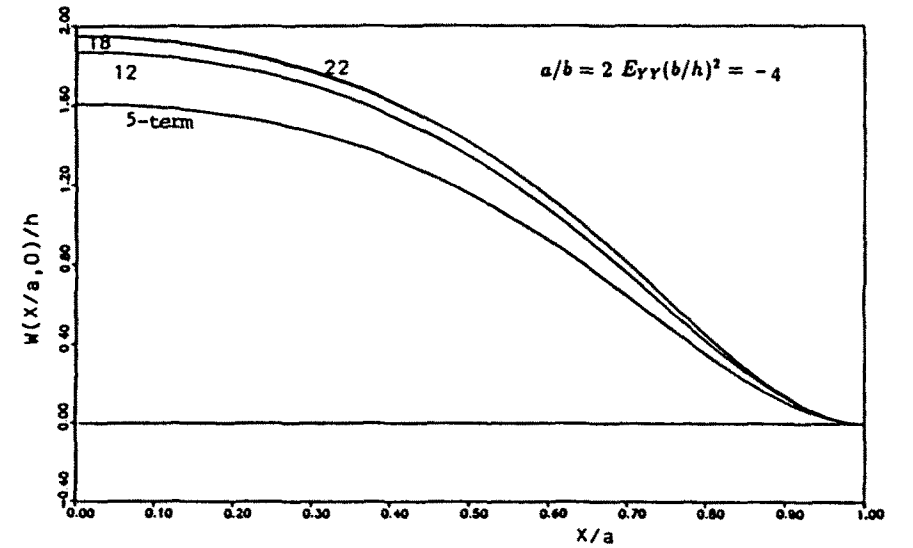

Fig. 11. Deflection profile along the X-axis ($a/b = 2$).

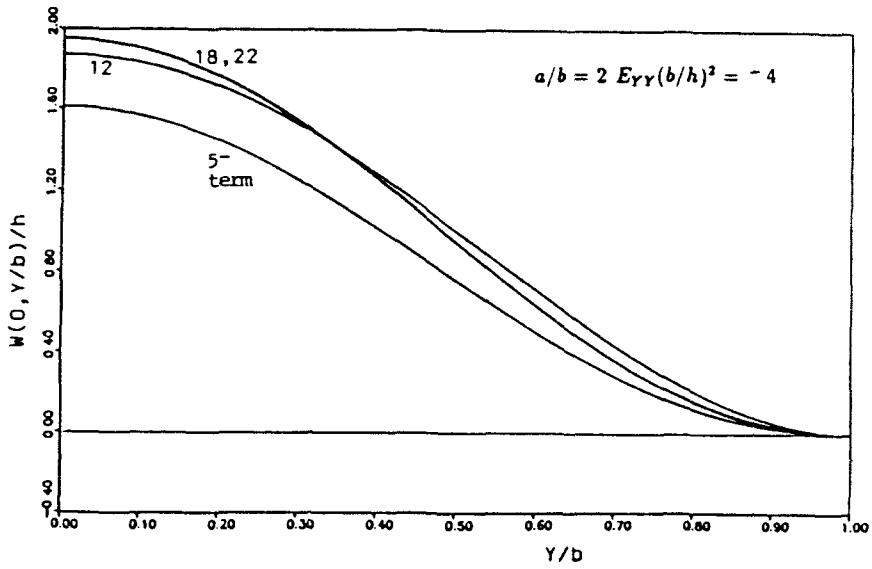

Fig. 12. Deflection profile along the Y-axis ($a/b = 2$).

Figure 11 indicates that, along the X-axis, the magnitude of the curvature of the deformed middle surface is smaller at the center of the plate and larger near the boundary points. Along the loading axis, the opposite is true (Fig. 12). Hence the normal bending moment is relatively small at the two ends of the loading axis and relatively large at the two ends of the X-axis. As the strain load increases, the concentration (attenuation) of the normal curvature and the bending moment at the end points of the X-axis (Y-axis) becomes more pronounced. This phenomenon has important implications on the postbuckling growth behavior of an elliptical delamination. Since the normal bending moment results in an opening action along the delamination boundary and contributes predominantly to the local energy release rate, delamination growth tends to initiate and continue along the X-axis until the boundary curvature and the moment at the two ends of the axis are sufficiently reduced by the lengthening of the X-axis. In addition, growth of the delamination along the X-direction exposes an interior strip around the Y-axis to states of deformation resembling those of one-dimensional delamination models, as may be seen by comparing the deflection profiles along the Y-axis for various (increasing) aspect ratios. Hence the curvature and the bending moment increase at the two ends of the Y-axis and, eventually, delamination growth may proceed simultaneously in both X- and Y-directions. The preceding reasoning provides an explanation for the initial transverse growth of a buckled two-dimensional delamination under a uniaxial in-plane compression, which has been observed experimentally (Chai *et al.*, 1983).

4.3. *Energy release rates*

The non-dimensionalized total potential energies associated with the preceding solutions are shown in Fig. 13. The results are shown as functions of the normalized strain load for elliptical delaminations with aspect ratios $a/b = 1$ and 10. At a large aspect ratio, the deviation of the results of the lowest order solution (Chai and Babcock, 1985) from the higher-order solutions becomes significant. The total potential energy may be differentiated with respect to the semi-axial length, a or b, to obtain the energy release rates associated with delamination growth along the X- or Y-directions. As the aspect ratio of the ellipse changes during the growth of the delamination, the energy release rate also varies. The results are presented in Figs 14 and 15, respectively, for delamination growth along the X- and Y-directions, and for three fixed values of the normalized strain load. It is clear that the lowest-order solution significantly underestimates the energy release rates.

The energy release rates calculated by differentiating the total potential energy with respect to the semi-axial lengths are global quantities associated with certain *assumed* modes

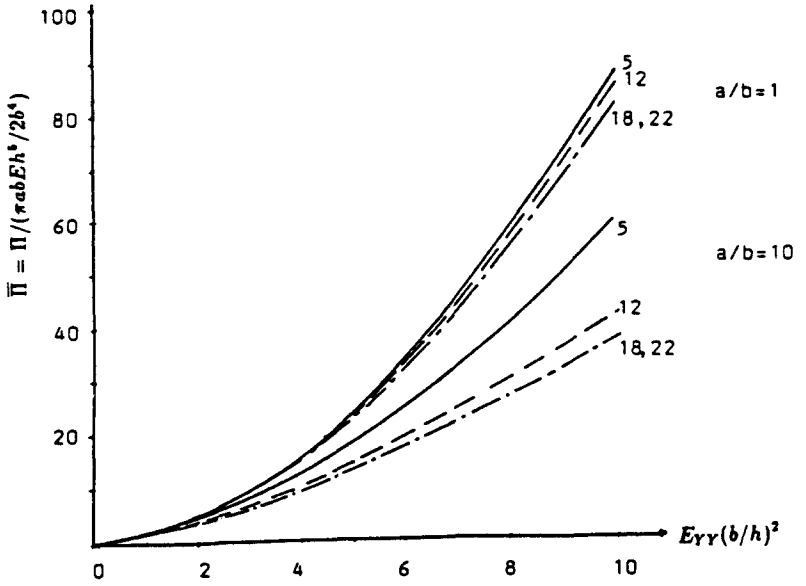

Fig. 13. Total potential energy versus the strain load.

of delamination growth. Although the shape of a two-dimensional delamination may be approximated by an ellipse in each stage of growth, the principal axes of the ellipse may rotate in the course of delamination growth if the loading axis does not coincide with the geometrical and material symmetry axes. Thus, the actual growth mode is generally not a combination of growth along two *fixed* principal directions and, strictly speaking, it can only be determined by evaluating the pointwise values of the energy release rate along the delamination boundary. Such local values of the energy release rate may be expressed in terms of the local membrane forces and bending moments. In the present case of an isotropic elliptical delaminated layer under biaxial loading, the maximum values of the energy release rate occur at the boundary points $(a, 0)$ and $(0, b)$. Figure 16 shows the normalized pointwise

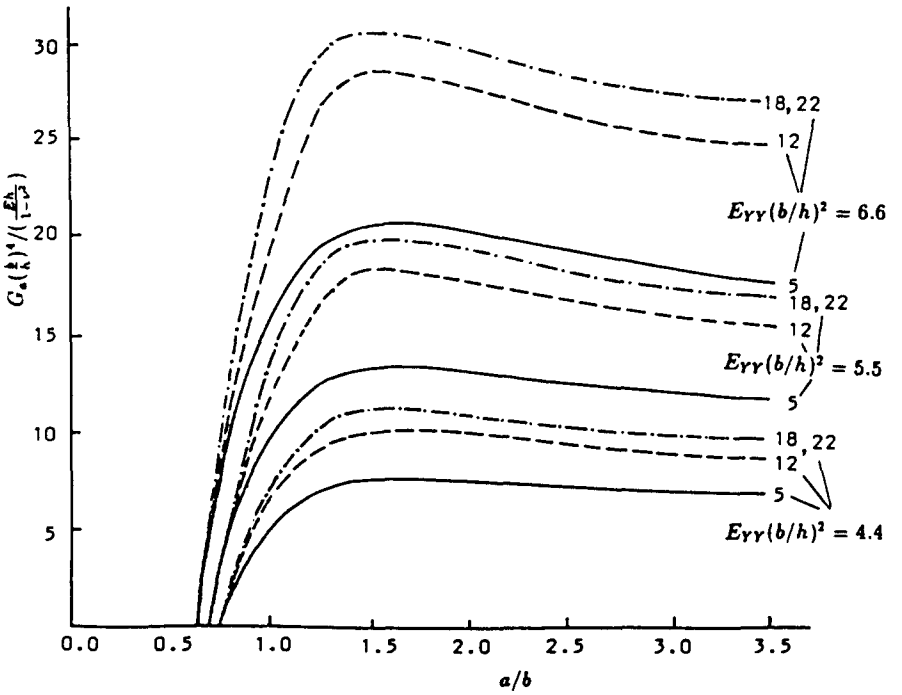

Fig. 14. Global energy release rate, delamination growth along the X-direction.

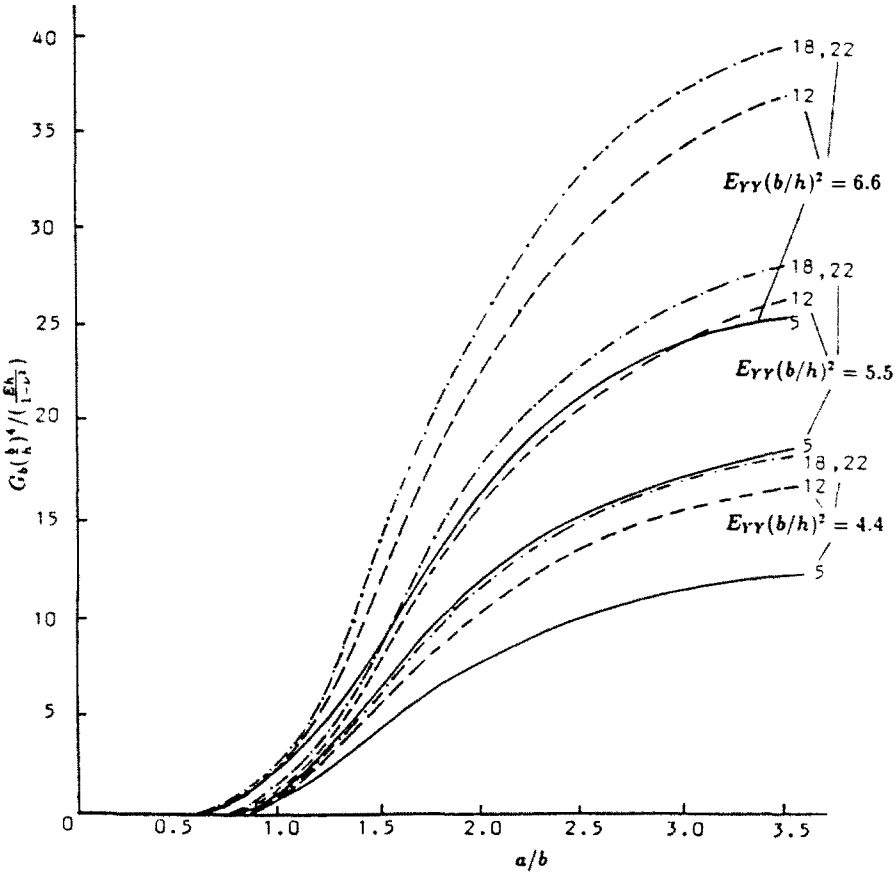

Fig. 15. Global energy release rate, delamination growth along the Y-direction.

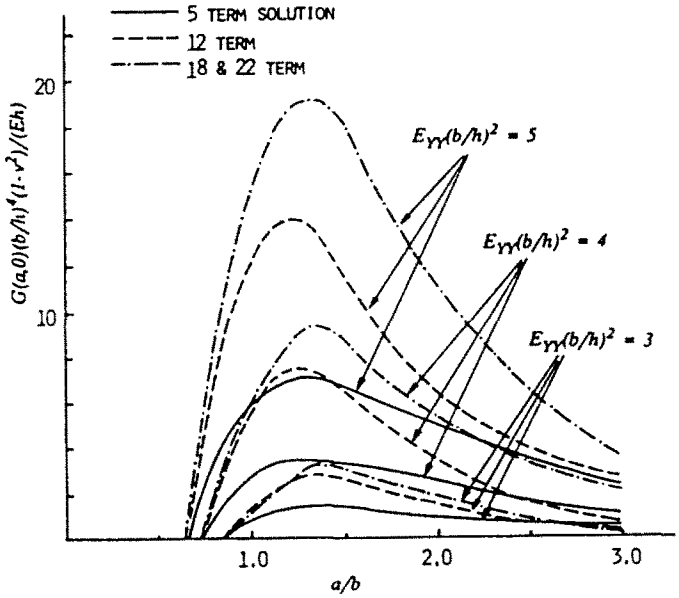

Fig. 16. Pointwise energy release rate at $(a, 0)$.

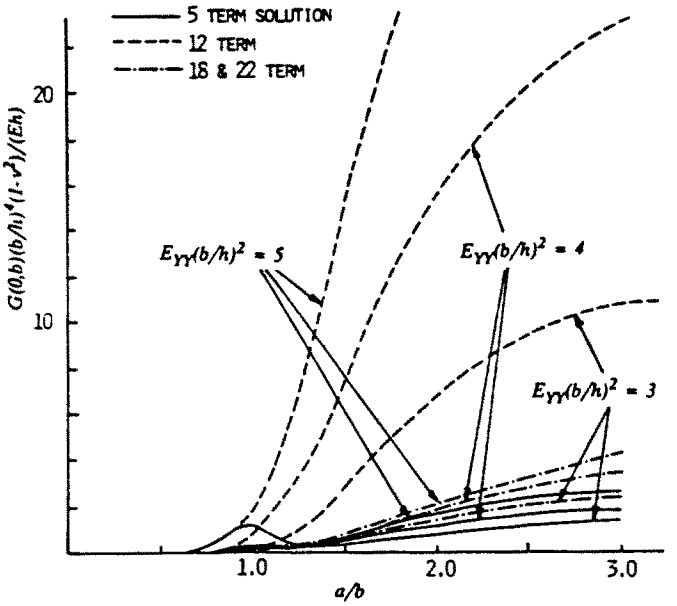

Fig. 17. Pointwise energy release rate at $(0, b)$.

energy release rate at $(a, 0)$ for three fixed levels of the strain load, and Fig. 17 shows the corresponding results at $(0, b)$. In Fig. 16, the solutions of the highest orders show the largest energy release rates, which are about twice as large as the results of the lowest-order solution. Figure 17 indicates that the solution of the order $\{3, 4\}$ greatly overestimates the pointwise energy release rate at $(0, b)$. These results suggest that solutions of the order lower than $\{5, 4\}$ cannot be used to predict the initiation and the nature of growth of a two-dimensional delamination. According to the highest-order solutions, the energy release rate at $(a, 0)$ consistently dominates over the rate at $(0, b)$ when the aspect ratio a/b is 3 or smaller. An opposite conclusion may be valid in the regime of large aspect ratios.

Some conclusions from the present buckling and postbuckling analysis of homogeneous isotropic elliptical sublaminates are summarized in Part II along with additional conclusions based on more extensive results for anisotropic cross-ply and angle-ply sublaminates.

Acknowledgements—The second author was supported by an Army Research Office grant to Georgia Institute of Technology in the autumn of 1988. The computational tasks of this project were made feasible by a grant for the use of Cyber 205 supercomputer from the Advanced Computational Methods Center, University of Georgia.

REFERENCES

Bodner, S. R. (1973). The postbuckling behavior of a clamped circular plate. *Quart. J. Appl. Math.* **12**, 397–401.
Bottega, W. J. (1983). A growth law for propagation of arbitrary shaped delamination in layered plates. *Int. J. Solids Structures* **19**, 1009–1017.
Chai, H. and Babcock, C. D. (1985). Two-dimensional modelling of compressive failure in delaminated laminates. *J. Comp. Mater.* **19**, 67–98.
Chai, H., Babcock, C. D. and Knauss, W. G. (1981). One dimensional modelling of failure in laminated plates by delamination buckling. *Int. J. Solids Structures* **17**, 1069–1083.
Chai, H., Knauss, W. G. and Babcock, C. D. (1983). Observation of damage growth in compressively loaded laminates. *Experimental Mech.* **23**, 329–337.
Chai, C. Y. (1980). *Nonlinear Analysis of Plates*. McGraw-Hill, New York.
Feng, M. (1983). An energy theory for postbuckling of composite plates under combined loading. *Comput. Struct.* **16**, 423–431.
Friedrichs, K. O. and Stoker, J. J. (1941). The non-linear boundary value problem of the buckled plate. *Amer. J. Math.* **63**, 839–888.
Friedrichs, K. O. and Stoker, J. J. (1942). Buckling of the circular plate beyond the critical thrust. *J. Appl. Mech.* **9**, 7–14.
Garg, A. C. (1988). Delamination—a damage mode in composite structures. *Engng Frac. Mech.* **29**, 557–584.
Jane, K. C. (1989). Buckling, postbuckling deformation and vibration of a delaminated plate. Ph.D. Thesis, Georgia Institute of Technology, Atlanta, GA.

Kapania, R. K. and Raciti, S. (1989). Recent advances in analysis of laminated beams and plates—Part I: Shear effects and buckling. *AIAA Jl* **27**, 923–934.

Shivakumar, K. N. and Whitcomb, J. D. (1985). Buckling of a sublaminate in a quasi-isotropic composite laminate. *J. Comp. Mater.* **19**, 2–18.

Simitses, G. J. (1989). Effect of delamination on buckling. In *Interlaminar Fracture in Composites* (Edited by E. A. Armanios), pp. 237–252. Trans Tech, Switzerland.

Storakers, B. (1989). Nonlinear aspects of delamination in structural members. In *Theoretical Mechanics* (Proc. XVIIth Int. Congr. Theor. Appl. Mech., Edited by P. Germain, M. Piau and D. Caillerie), pp. 315–336. Elsevier, New York.

Storakers, B. and Anderson, B. (1988). Nonlinear plate theory applied to delamination in composites. *J. Mech. Phys. Solids* **36**, 689–718.

Woinowsky-Krieger, S. (1937). The stability of a clamped elliptical plate under uniform compression. *J. Appl. Mech.* **4**, 177–178.

Yin, W.-L. (1985). Axisymmetric buckling and growth of a circular delamination in a compressed laminate. *Int. J. Solids Structures* **21**, 503–514.

Yin, W.-L. (1989). Recent analytical results in delamination buckling and growth. In *Interlaminar Fracture in Composites* (Edited by E. A. Armanios), pp. 253–266. Trans Tech, Switzerland.

Yin, W.-L., Reddy, A. D., Dorris, W. S. and Biggers, S. B. (1986a). Delamination buckling and growth in a laminated beam plate with and without stiffening. Final Report, Task I, NAS1-17925, Lockheed-Georgia Company, Marietta, GA.

Yin, W.-L., Sallam, S. N. and Simitses, G. J. (1986b). Ultimate axial load capacity of a delaminated beam-plate. *AIAA Jl* **24**, 123–128.

Yin, W.-L. and Wang, J. T. S. (1984). The energy release rate in the growth of a one-dimensional delamination. *J. Appl. Mech.* **51**, 939–941.